SU-4240-648(revised)
hep-th/9712247
April,1997

Anomalous Defects and Their Quantized Transverse Conductivities

A.P. Balachandran, Varghese John, Arshad Momen

Department of Physics, Syracuse University,

Syracuse, NY 13244-1130, U.S.A.

Fernando Moraes

Departamento de Fisica,

Universidade Federal de Pernambuco,

50670-901 Recife, PE, Brazil.

Abstract

Using a description of defects in solids in terms of three-dimensional gravity, we study the propagation of electrons in the background of disclinations and screw dislocations. We study the situations where there are bound states that are effectively localized on the defect and hence can be described in terms of an effective $1+1$ dimensional field theory for the low energy excitations. In the case of screw dislocations, we find that these excitations are chiral and can be described by an effective field theory of chiral fermions. Fermions of both chirality occur even for a given direction of the magnetic field. The "net" chirality of the system however is not always the same for a given direction of the magnetic field, but changes from one sign of the chirality through zero to the other sign as the Fermi momentum or the magnitude of the magnetic flux

is varied. On coupling to an external electromagnetic field, the latter becomes anomalous, and predicts novel conduction properties for these materials.

I. INTRODUCTION

The effect of defects on properties of solids has been a very active field of research [1]. The fact that the theory of defects in solids can be reformulated as a version of three-dimensional gravity has been discussed in [2]. This formulation corresponds to looking at the continuum limit of a crystalline solid in which the static defect configuration is characterized by a non-trivial metric corresponding to a static spacetime. There is a one-to-one correspondence between the classification of defects in terms of Burgers vectors and different metric configurations. This formulation has the merit of highlighting the geometrical properties of defect configurations.

The properties of electrons interacting with these static defects can be studied by looking at their propagation in the background of these defects [3]. In this paper, we will focus on situations where one can have bound states of electrons localized on line defects like the disclination and the screw dislocation. In this context, it is useful to recall that there is a very close similarity of this system to that of particles in the background of cosmic strings and domain walls [4,5]. It is known that there exist states localized on strings and domain walls, leading to interesting phenomena like gauge and gravitational anomalies. The properties of states localized on domain walls in the context of condensed matter systems have also been studied in [6,7].

As mentioned above, we here study situations where there are bound states localized on line defects. In cases where one has chiral bound states, the effective description of low lying excitations at the defects is given in terms of a $(1 + 1)$ dimensional massless chiral Dirac fermion theory. Using well-known results about the gauge theory of chiral fermions in $(1 + 1)$ dimensions, one can show that there is a $U(1)$ anomaly [8], leading to charge

nonconservation in the $(1+1)$ dimensional effective action. One can also show that the charge nonconservation is exactly cancelled by the neglected bulk modes [9]. These modes contribute to the bulk current. The latter leads to a net inflow of charge to the defect that precisely accounts for the charge violation given by the $U(1)$ anomaly. This effect of the bulk modes can be summarized in terms of effective Chern-Simons actions on planes having the defect as boundary.

In order to give a simple but explicit example of the above scenario, we first study the Schrödinger equation of the electron in an external electromagnetic field in the absence of any defect. The coupling of the latter to the magnetic moment of the electron is also taken into account. We assume that the gyromagnetic ratio of the electron is two. In this case, it is known that the Dirac Hamiltonian in two dimensions can be squared to obtain the Schrödinger equation with magnetic moment interaction. The corresponding two dimensional (2d) Schrödinger Hamiltonian is the part of the 3d Schrödinger Hamiltonian transverse to the defect. We first analyze the 2d Dirac Hamiltonian and its domains of self-adjointness. The latter are found to be compatible with the domains for the 2d Schrödinger Hamiltonian when the derivatives of the Dirac wave function are in the same domain as the wave function itself.

In the absence of defects, the above 2d Dirac equation and the corresponding 2d Schrödinger equation are known to have bound states of zero energy. The number of bound states is given by an index theorem and is related to the integer part of the flux through the plane. This is the Aharonov-Casher theorem [10]. These bound states are localized in the region of the magnetic field.

We extend the Aharonov-Casher analysis to situations where there are special types of defects, namely the edge disclination and the screw dislocation. We find that similar results exist in this situation, that is we can extend the counting of bound states to the situation where there is a conical deficit angle and a screw defect.

Next we obtain a $(1+1)$ dimensional field theory for the bound states as they move along the defect by linearizing the excitations about the Fermi surface. It is a $(1+1)$-dimensional

chiral fermion theory for the low energy excitations. When this effective field theory is coupled to an external electromagnetic field, there is then an anomaly [8]. We then proceed to look at the response of the system to a constant electric field applied in the direction of the defect and find that there is a net inflow of charge from the planes transverse to the defect, in other words a "transverse Hall effect", because of the anomaly.

The paper is arranged as follows. In section 2, we discuss the problem of the motion of an electron on a plane (with or without a point removed) in an external magnetic field and find the Dirac Hamiltonian. In section 3, we do the partial-wave analysis for this Hamiltonian when the plane has a hole and find its domains of self-adjointness. We also find the zero-energy solutions for the Dirac Hamiltonian. We introduce the line defects, namely disclinations and screw defects, in section 4. We also find the zero energy solutions in these background geometries, which are very similar to their flat space counterparts. These states turn out to be individually chiral in terms of their motion around the defect, specifically, the screw defect. However, the total chirality of the system however is not always the same for a given direction of the magnetic field, but changes from one sign of the chirality through zero to the other sign as the Fermi momentum or the magnitude of the magnetic flux is varied. In section 5, we write the (1+1)-dimensional effective field theory for these chiral states and couple it to an external electric field along the defect. This theory is anomalous as discussed above. This anomaly allows one to find the effective field theory in the bulk of the medium where the defect is embedded. It is given by Chern-Simons terms defined on the half-planes which have the line defect as the boundary. Finally, in the concluding section 6, we discuss other physical effects that can be deduced using this reformulation of defects in terms of non-trivial metric solutions of the gravitational equations.

II. THE HAMILTONIAN ON THE PLANE

In this section we will be discussing the motion of an electron in an external magnetic field along the z-direction. We will consider the Schrödinger equation for a spin half particle

with a magnetic moment interaction in this ambient space.

The line element describing the Euclidean geometry of $\mathbb{R}^3$ is given by

$$ds^2 = (dr^2 + r^2 d\theta^2) + dz^2, \tag{2.1}$$

r, θ, z being the cylindrical coordinates. We will see later that various defect geometries can also be described by line elements like the above one.

The spatial Laplacian is

$$\Delta = [\frac{1}{r}\frac{\partial}{\partial r}(r\frac{\partial}{\partial r}) + \frac{1}{r^2}\frac{\partial^2}{\partial \theta^2} + \frac{\partial^2}{\partial z^2}] \ . \tag{2.2}$$

We now split Δ according to

$$\Delta = \Delta_T + \Delta_Z = \Delta_T + \frac{\partial^2}{\partial z^2}. \tag{2.3}$$

In the presence of a magnetic field along the z-direction and also a magnetic moment interaction, the electronic wavefunction on the plane satisfies the Pauli equation

$$(-\frac{1}{2m^*}\bar{\Delta}_T - \frac{\mu}{2}\sigma \cdot B)\Psi = E\Psi \tag{2.4}$$

where $\bar{\Delta}_T = D_i D_i$ is the transverse Laplacian constructed from the gauge-covariant derivative

$$D_i \equiv \partial_i - iA_i \ , \tag{2.5}$$

and μ and m^* are the electronic magnetic moment and effective mass respectively. Notice that we have chosen our units by requiring the electronic charge e to be 1. We have also chosen a gauge where $A_0 = 0$.

When $\mu = \frac{1}{m^*}$, the Hamiltonian in (2.4) can be obtained by squaring the two-dimensional massless Dirac Hamiltonian. We will be dealing with this Dirac Hamiltonian below.

For regular Cartesian coordinates our choice of the γ matrices are

$$\gamma^t \equiv \gamma^0 = \sigma_3; \qquad \gamma^x = -i\sigma_2; \qquad \gamma^y = i\sigma_1, \tag{2.6}$$

where σ_i are the standard Pauli matrices. From here one can readily find the γ matrices for the polar basis :

$$\gamma^0 = \sigma_3, \qquad \gamma^1 = (\boldsymbol{\gamma}\cdot\hat{\boldsymbol{r}}) = \begin{pmatrix} 0 & -e^{-i\theta} \\ e^{i\theta} & 0 \end{pmatrix}, \qquad \gamma^2 = (\boldsymbol{\gamma}\cdot\hat{\boldsymbol{\theta}}) = \begin{pmatrix} 0 & ie^{-i\theta} \\ ie^{i\theta} & 0 \end{pmatrix}. \tag{2.7}$$

We assume that B is time-independent. We can then choose a gauge where both A_0 and A_r are zero. In this gauge, the transverse Dirac Hamiltonian is identified via the equation $i\frac{\partial}{\partial t}\Psi = H_D\Psi$ where

$$\begin{aligned} H_D &= -i\gamma^0(\gamma^x D_x + \gamma^y D_y) \\ &= \gamma^0[-i(\boldsymbol{\gamma}\cdot\hat{\boldsymbol{r}})\partial_r - i\frac{1}{r}(\boldsymbol{\gamma}\cdot\hat{\boldsymbol{\theta}})(\partial_\theta - irA_\theta)] \\ &= \begin{pmatrix} 0 & ie^{-i\theta}\left[\frac{\partial}{\partial r} + \frac{1}{r}(-i\frac{\partial}{\partial\theta} - rA_\theta)\right] \\ ie^{i\theta}\left[\frac{\partial}{\partial r} - \frac{1}{r}(-i\frac{\partial}{\partial\theta} - rA_\theta)\right] & 0 \end{pmatrix}. \end{aligned} \tag{2.8}$$

This Hamiltonian is formally symmetric with respect to the measure $r\ dr\ d\theta$.

Squaring this operator leads to the Hamiltonian (2.4) with $\mu = \frac{1}{m^*}$:

$$H = \frac{1}{2m^*}H_D H_D. \tag{2.9}$$

Next we proceed to study the boundary conditions at the defect at $r = 0$ appropriate for this Dirac operator.

III. THE DIRAC EQUATION ON $\mathbb{R}^2 - \{0\}$

The massless Dirac equation on a plane with a point removed admits a one-parameter family of boundary conditions at $r = 0$. This can be seen as follows.

The Dirac operator $-i\boldsymbol{\sigma}\cdot\boldsymbol{\nabla}_T$ defined (in the absence of the magnetic field) on the two-dimensional plane, is self-adjoint on a domain $\mathcal{D}$ if and only if [11]

$$\int_0^\infty r dr \int_0^{2\pi} d\theta \left[\boldsymbol{\chi}^\dagger\{-i\boldsymbol{\sigma}\cdot\boldsymbol{\nabla}_T\Psi\} - \{-i\boldsymbol{\sigma}\cdot\boldsymbol{\nabla}_T\boldsymbol{\chi}\}^\dagger\Psi\right] = 0$$
$$\text{for} \quad \Psi \in \mathcal{D} \Leftrightarrow \boldsymbol{\chi} \in \mathcal{D}, \tag{3.1}$$

where

$$\boldsymbol{\nabla}_T \equiv \hat{\boldsymbol{r}}\frac{\partial}{\partial r} + \hat{\boldsymbol{\theta}}\frac{1}{r}\frac{\partial}{\partial \theta}. \tag{3.2}$$

Using Stokes' theorem and assuming that the wavefunctions fall off appropriately at spatial infinity, one ends up with the following equation at the boundary (at $r = 0$):

$$\lim_{r\to 0}\int d\theta \;\; r\boldsymbol{\chi}^\dagger \mathcal{A}\; \Psi = 0 \qquad \text{for} \;\; \Psi \in \mathcal{D} \Leftrightarrow \boldsymbol{\chi} \in \mathcal{D}. \tag{3.3}$$

Here,

$$\mathcal{A} \equiv -i\boldsymbol{\sigma}\cdot\hat{\boldsymbol{r}} = \begin{pmatrix} 0 & -ie^{-i\theta} \\ -ie^{i\theta} & 0 \end{pmatrix}. \tag{3.4}$$

The eigenvalues of the operator $\mathcal{A}$ are $+i$ and $-i$ and the corresponding eigenvectors normalized to 1 are

$$\frac{1}{\sqrt{2}}\begin{pmatrix} 1 \\ -e^{i\theta} \end{pmatrix}, \qquad \text{and} \qquad \frac{1}{\sqrt{2}}\begin{pmatrix} 1 \\ e^{i\theta} \end{pmatrix} \tag{3.5}$$

respectively. It follows that the boundary conditions at $r = 0$ compatible with self-adjointness of $-i\boldsymbol{\sigma}\cdot\boldsymbol{\nabla}_T$ are parametrized by $e^{iK} \in U(1)$ [K being real] and are given by

$$\lim_{r\to 0}\sqrt{r}\Psi(r,\theta) \equiv \begin{pmatrix} \psi_1 \\ \psi_2 \end{pmatrix}(0,\theta) = \alpha(\theta)\left[\begin{pmatrix} 1 \\ e^{i\theta} \end{pmatrix} + e^{iK}\begin{pmatrix} 1 \\ -e^{i\theta} \end{pmatrix}\right], \tag{3.6}$$

where $\alpha(\theta)$ is any smooth function on S^1. The parameter K (mod 2π) parametrizes the various boundary conditions. One can readily see that in terms of K,

$$\cos(\frac{K}{2})\psi_2(0,\theta) = -ie^{i\theta}\sin(\frac{K}{2})\psi_1(0,\theta). \tag{3.7}$$

When K is 0 or π, this shows that the components $\psi_2(0,\theta)$ or $\psi_1(0,\theta)$ vanish respectively and the solutions turn out to be "chiral" at the origin.

It is important that the Laplacian remains self-adjoint under the chosen conditions. We must therefore augment (3.6) by the same types of boundary condition on the radial derivatives too,

$$\lim_{r\to 0}\sqrt{r}\partial_r\Psi(r,\theta)=\beta(\theta)\left[\begin{pmatrix}1\\ e^{i\theta}\end{pmatrix}+e^{iK}\begin{pmatrix}1\\ -e^{i\theta}\end{pmatrix}\right]. \tag{3.8}$$

Here $\beta(\theta)$ is any smooth function on S^1. [It need not be $\alpha(\theta)$.] Equations (3.6) and (3.8) lead to

$$\int r dr\, d\theta\left[\boldsymbol{\chi}^\dagger\Delta_T\Psi-(\Delta_T\boldsymbol{\chi})^\dagger\Psi\right]=\lim_{r\to 0}\int r\ d\theta[(\chi_1^\dagger\partial_r\psi_1+\chi_2^\dagger\partial_r\psi_2)-(\partial_r\chi_1^\dagger\psi_1+\partial_r\chi_2^\dagger\psi_2)]=0$$
$$\text{for}\quad \Psi\in\mathcal{D}\Leftrightarrow\boldsymbol{\chi}\in\mathcal{D}. \tag{3.9}$$

Here $\mathcal{D}\equiv\mathcal{D}(e^{iK})$ is the set of functions fulfilling both the conditions (3.6) and (3.8). Thus the Laplacian is also self-adjoint with (3.6) and (3.8).

We now include the magnetic field. It can easily be checked that the self-adjointness conditions discussed above remain unaffected as long as we are not dealing with singular magnetic field configurations.

We will assume that our magnetic field is non-vanishing only over a compact region enclosing the defect. For simplicity we will in fact assume that the magnetic field is a constant within a circle of radius a and zero outside. (The magnetic field can be represented by a delta function in the limit of $a=0$, this case has been treated in detail by Moroz [12].) Hence, our vector potential will be chosen to have the form

$$\begin{aligned}
&A=A_r dr+A_\theta r d\theta,\\
&A_r=0,\qquad\qquad A_\theta=\frac{Br}{2}\tilde{\theta}(a-r)+\frac{\Phi}{2\pi r}\tilde{\theta}(r-a),\\
&dA\equiv B_z r dr\ d\theta=B\tilde{\theta}(a-r)d^2x=B\tilde{\theta}(a-r)\ r dr d\theta
\end{aligned} \tag{3.10}$$

where

$$\Phi=\pi a^2 B \tag{3.11}$$

is the total flux and $\tilde{\theta}$ the step function. [We denote it by $\tilde{\theta}$ to avoid duplication of notation.]

As the magnetic field is cylindrically symmetric, the angular momentum for the Dirac particle is a good quantum number. Accordingly, the conditions (3.6) and (3.8) can by analyzed in terms of the simultaneous eigenfunctions of H_D and the total angular momentum operator $J = L + \frac{1}{2}\sigma_3$ where $L = -i\frac{\partial}{\partial\theta}$ is the orbital angular momentum operator. The eigenfunction of the Dirac Hamiltonian H_D with total angular momentum j has the form

$$\Psi_j(r,\theta) = \begin{pmatrix} e^{i(j-\frac{1}{2})\theta}u_j(r) \\ e^{i(j+\frac{1}{2})\theta}v_j(r) \end{pmatrix} \equiv \begin{pmatrix} e^{im\theta}u_{m+\frac{1}{2}}(r) \\ e^{i(m+1)\theta}v_{m+\frac{1}{2}}(r) \end{pmatrix} , \tag{3.12}$$

where $m = j - \frac{1}{2}$. In terms of $u_{m+\frac{1}{2}}$ and $v_{m+\frac{1}{2}}$, the boundary condition (3.7) reads as

$$\sqrt{r}\cos(\frac{K}{2})v_{m+\frac{1}{2}}(r) = \sqrt{r}\sin(\frac{K}{2})u_{m+\frac{1}{2}}(r). \tag{3.13}$$

The spectrum of angular momentum depends on the (quasi-)periodicity of the wave function under the $\theta \to \theta + 2\pi$ translation,

$$\Psi(r,\theta+2\pi) = e^{i\lambda}\Psi(r,\theta) \tag{3.14}$$

which implies that

$$m \in \frac{\lambda}{2\pi} + n, \qquad n \in \mathbb{Z}. \tag{3.15}$$

The Hamiltonian H_D, restricted to the m-th partial wave $\Psi_m(r) \equiv \begin{pmatrix} u_{m+\frac{1}{2}} \\ v_{m+\frac{1}{2}} \end{pmatrix}$, acquires the form

$$\begin{aligned} H_D^{(m)} &= \begin{pmatrix} 0 & i\left[\frac{\partial}{\partial r} + \frac{1}{r}(m+1-rA_\theta)\right] \\ i\left[\frac{\partial}{\partial r} - \frac{1}{r}(m-rA_\theta)\right] & 0 \end{pmatrix} \\ &\equiv \begin{pmatrix} 0 & D \\ D^\dagger & 0 \end{pmatrix} . \end{aligned} \tag{3.16}$$

On squaring $H_D^{(m)}$, one obtains the Schrödinger operators

$$\begin{aligned} DD^\dagger &= -\bar{\Delta}_T^{(m)} - B_z, \\ D^\dagger D &= -\bar{\Delta}_T^{(m+1)} + B_z, \\ B_z &\equiv \frac{1}{r}\partial_r(rA_\theta), \end{aligned} \tag{3.17}$$

$\Delta_T^{(m)}$ being the radial Laplacian including the gauge connection (which is a function of r only),

$$\Delta_T^{(m)} = \frac{\partial^2}{\partial r^2} + \frac{1}{r}\frac{\partial}{\partial r} - \frac{(m - rA_\theta)^2}{r^2} \tag{3.18}$$

and B_z is the component of the magnetic field in the third direction, that is, in the direction normal to the plane.

We now proceed to find zero energy solutions of the Dirac equation satisfying the boundary condition (3.6). They automatically satisfy the boundary condition (3.8) and hence are zero energy solutions of the Laplacian too.

For a generic A_θ, the zero energy eigenfunctions of $H_D^{(m)}$ [ignoring the boundary condition (3.13) and square integrability for the moment] are given by

$$\Psi_m(r) = \begin{pmatrix} Cr^m e^{-\int_0^r A_\theta(r')dr'} \\ Dr^{-(m+1)} e^{\int_0^r A_\theta(r')dr'} \end{pmatrix} \tag{3.19}$$

There is a bound on the value of m from the requirement of square integrability of the eigenfunctions. Let us assume that Φ is positive (i.e. the magnetic field is pointing along positive z-axis). Using the asymptotic forms

$$\int_0^r A_\theta(r')dr' = \begin{cases} 0 & \text{as } r \to 0, \\ \frac{\Phi}{2\pi}\ln r & \text{as } r \to \infty \end{cases} \tag{3.20}$$

which follow from (3.10), the solutions (3.19), the condition (3.13) and the requirements of square-integrability of the wavefunctions at $r = 0$ and $r \to \infty$, we obtain the wave function

$$\Psi_m(r) = \begin{pmatrix} Cr^m e^{-\int_0^r A_\theta(r')dr'} \\ 0 \end{pmatrix} \tag{3.21}$$

and the following bounds on m :

$$\begin{aligned} &\text{a) When } e^{iK} \neq 1 \quad : \qquad -\frac{1}{2} < m < (\frac{\Phi}{2\pi} - 1), \\ &\text{b) When } e^{iK} = 1 \quad : \qquad -\frac{1}{2} \leq m < (\frac{\Phi}{2\pi} - 1). \end{aligned} \tag{3.22}$$

These bounds imply that

$$\Phi > \pi. \tag{3.23}$$

Thus, there are about $[\frac{\Phi}{2\pi} - \frac{1}{2}]$ independent spin polarized zero energy solutions, $[\xi]$ denoting the largest integer not exceeding ξ. [The precise number depends on the value of e^{iK} and the allowed values of m.] It is important to note that the parameter K determines whether the mode $m = -\frac{1}{2}$ is a bound state or not. Of course this value of m is allowed only if that $\lambda = \pi(\mathrm{mod}2\pi)$ as well.

On the other hand, when Φ is negative, we find the wave function

$$\Psi_m(r) = \begin{pmatrix} 0 \\ Dr^{-(m+1)} e^{\int_0^r A_\theta(r')dr'} \end{pmatrix} \tag{3.24}$$

where m is now bounded as follows:

$$\begin{aligned} &\text{c) When } e^{iK} \neq -1 \quad : \qquad -\frac{1}{2} > m > \frac{\Phi}{2\pi}, \\ &\text{d) When } e^{iK} = -1 \quad : \qquad -\frac{1}{2} \geq m > \frac{\Phi}{2\pi}. \end{aligned} \tag{3.25}$$

As a consequence,

$$\Phi < -\pi. \tag{3.26}$$

Note that no zero energy bound states exist when $\Phi \leq |\pi|$.

We next proceed to extend this analysis to three dimensions and in particular to dislocations and screw defects.

IV. DISCLINATION AND SCREW DISLOCATION

A. Disclination

The above analysis can be extended very easily to the case when we have a conical defect or a screw dislocation in our background. In the presence of a conical defect (which one

can create by simply cutting out a wedge from a plane and identifying [pasting together] the edges or by inserting a wedge), the geometry of the defect can be represented by the metric [2]

$$ds^2 = (dr^2 + \alpha^2 r^2 d\theta^2) + dz^2 \tag{4.1}$$

where the coordinates r, θ, z are the standard cylindrical coordinates [with $\theta = 0$ and $\theta = 2\pi$ being identified as usual] and $2\pi(1-\alpha)$ is the opening angle of the cutout wedge. Note that $0 \leq \alpha \leq 1$. In this coordinate system, the Laplacian can be written as

$$\Delta = \frac{1}{r}\frac{\partial}{\partial r}(r\frac{\partial}{\partial r}) + \frac{1}{\alpha^2 r^2}\frac{\partial^2}{\partial \theta^2} + \frac{\partial^2}{\partial z^2} \ . \tag{4.2}$$

It is convenient to rescale the coordinates as follows :

$$\begin{aligned} r &\rightarrow R = r, \\ \theta &\rightarrow \Theta = \alpha\theta, \\ z &\rightarrow Z = z. \end{aligned} \tag{4.3}$$

The Laplacian then becomes

$$\tilde{\Delta} = [\frac{1}{R}\frac{\partial}{\partial R}(R\frac{\partial}{\partial R}) + \frac{1}{R^2}\frac{\partial^2}{\partial \Theta^2} + \frac{\partial^2}{\partial Z^2}]. \tag{4.4}$$

Although $\tilde{\Delta}$ looks like the flat space Laplacian, the range of Θ is different, $0 \leq \Theta \leq 2\pi\alpha$. As a consequence, the (quasi)periodicity of the wavefunction now reads

$$\Psi(R, \Theta + 2\pi\alpha) = e^{i\lambda}\Psi(R, \Theta). \tag{4.5}$$

We also demand the identical periodicity condition on the radial derivative to ensure that $\tilde{\Delta}$ is self-adjoint.

For the condition (4.5), the spectrum of the "angular momentum" $-i\frac{\partial}{\partial\Theta}$ gets quantized in units of $\frac{1}{\alpha}(m + \frac{\lambda}{2\pi})$, where $m \in \mathbb{Z}^+$. The method of counting the bound states is the same as in section 3, but for the change $m \rightarrow \frac{m}{\alpha}$. This incidentally also shows that the number of bound states can change in the presence of a disclination.

B. Screw Dislocation

Next we move on to the screw dislocation. The screw dislocation can be characterized by the metric

$$\begin{aligned} ds^2 &= (dr^2 + \alpha^2 r^2 d\theta^2) + (dz + \beta d\theta)^2 \equiv g_{ij} d\xi^i d\xi^j, \\ d\xi^1 &= dr, \quad d\xi^2 = d\theta, \quad d\xi^3 = dz \end{aligned} \tag{4.6}$$

where as usual r, θ, z are the cylindrical coordinates for $\mathbb{R}^3$.

The matrix $[g_{ij}]$ and its inverse $[g^{ij}]$ can be written as

$$[g_{ij}] = \begin{pmatrix} 1 & 0 & 0 \\ 0 & (\alpha^2 r^2 + \beta^2) & \beta \\ 0 & \beta & 1 \end{pmatrix}, \qquad \left[g^{ij}\right] = \begin{pmatrix} 1 & 0 & 0 \\ 0 & \frac{1}{\alpha^2 r^2} & \frac{-\beta}{\alpha^2 r^2} \\ 0 & \frac{-\beta}{\alpha^2 r^2} & (1 + \frac{\beta^2}{\alpha^2 r^2}) \end{pmatrix} \tag{4.7}$$

respectively.

The Laplacian after a rescaling as in (4.3) is

$$\begin{aligned} \Delta_1 &= \frac{1}{\sqrt{g}} \partial_i (g^{ij} \sqrt{g} \partial_j) \\ &= [\frac{1}{R}(\frac{\partial}{\partial R} R \frac{\partial}{\partial R}) + \frac{1}{R^2}(\frac{\partial}{\partial \Theta} - \frac{\beta}{\alpha}\frac{\partial}{\partial Z})^2 + \frac{\partial^2}{\partial Z^2}], \\ g &\equiv det[g_{ij}]. \end{aligned} \tag{4.8}$$

Wave functions in the domain of this Laplacian fulfill (3.7).

It may be emphasized here that in the presence of a screw defect, the geodesics of the metric $[g_{ij}]$ give the free propagation of low energy electrons.[1]

---

[1]By making the coordinate change $Z \to Z' = Z + \frac{\beta}{\alpha}\Theta$, this problem can be mapped into that of a Laplacian on flat space, but with a non-trivial boundary condition. Specifically, the quasi-periodicity of the wavefunction under $\Theta \to \Theta + 2\pi\alpha$ translates into

$$\Psi(R, \Theta, Z') = e^{i\lambda} \Psi(R, \Theta + 2\pi\alpha, Z' + 2\pi\beta).$$

Next we add a magnetic field in the Z-direction. This is done as before, by replacing ∂_i by $\partial_i - iA_i$ where $A_R = 0; A_\Theta = \frac{1}{\alpha}[\tilde{\theta}(a-R)\frac{BR}{2} + \frac{\Phi}{2\pi R}\tilde{\theta}(R-a)]$ and also introducing a magnetic moment interaction. Note that the potential has been suitably scaled so that the total flux is still Φ. The Hamiltonian then reads

$$H = -\frac{1}{2m^*}[\frac{1}{R}\frac{\partial}{\partial R}(R\frac{\partial}{\partial R}) + \frac{1}{R^2}\mathcal{D}_\Theta^2 + \frac{\partial^2}{\partial Z^2}] - \frac{1}{2m^*}\boldsymbol{\sigma}\cdot\boldsymbol{B} \tag{4.9}$$

where $\mathcal{D}_\Theta = (\partial_\Theta - iRA_\Theta - \frac{\beta}{\alpha}\partial_Z)$.

The zero energy eigenfunctions of H are found as before, by first splitting H into a transverse part and a part along the Z-direction. The transverse Hamiltonian

$$H_T = -\frac{1}{2m^*}[\frac{1}{R}\frac{\partial}{\partial R}(R\frac{\partial}{\partial R}) + \frac{1}{R^2}\mathcal{D}_\Theta^2] - \frac{1}{2m^*}\boldsymbol{\sigma}\cdot\boldsymbol{B} \tag{4.10}$$

is still expressible as a square of a Dirac operator,

$$\begin{aligned} H_T &= \frac{1}{2m^*}\begin{pmatrix} \tilde{D}\tilde{D}^\dagger & 0 \\ 0 & \tilde{D}^\dagger\tilde{D} \end{pmatrix} = \frac{1}{2m^*}H_{\tilde{D}}^2, \\ H_{\tilde{D}} &= \begin{pmatrix} 0 & \tilde{D} \\ \tilde{D}^\dagger & 0 \end{pmatrix} \end{aligned} \tag{4.11}$$

where

$$\begin{aligned} \tilde{D} &= ie^{-i\Theta}[\frac{\partial}{\partial R} - \frac{i}{R}\mathcal{D}_\Theta], \\ \tilde{D}^\dagger &= ie^{i\Theta}[\frac{\partial}{\partial R} + \frac{i}{R}\mathcal{D}_\Theta]. \end{aligned} \tag{4.12}$$

Requiring that $\tilde{D}$ and $\tilde{D}^\dagger$ be the adjoint of each other (so that $H_{\tilde{D}}$ is self-adjoint) leads once again to the same boundary conditions (3.6).

We will make the ansatz that the wavefunction is of the form

$$\Psi = \psi_T e^{ikZ}. \tag{4.13}$$

Now, the zero energy modes of $H_{\tilde{D}}$ (and hence those of H_T) [ignoring the boundary condition at the origin and square integrability for the moment] are given (up to an overall normalization factor) by

$$\psi_T = \begin{pmatrix} CR^m e^{-\int_0^R A_\Theta(r')dr'} e^{i(m+\frac{\beta}{\alpha}k)\Theta} \\ DR^{-(m+1)} e^{\int_0^R A_\Theta(r')dr'} e^{i(m+\frac{\beta}{\alpha}k+1)\Theta} \end{pmatrix}. \tag{4.14}$$

The corresponding functions for the full Hamiltonian (4.9) are plane waves along the Z-direction and are given by

$$\Psi = \begin{pmatrix} CR^m e^{-\int_0^R A_\Theta(r')dr'} e^{i(m+\frac{\beta}{\alpha}k)\Theta} e^{ikZ} \\ DR^{-(m+1)} e^{\int_0^R A_\Theta(r')dr'} e^{i(m+\frac{\beta}{\alpha}k+1)\Theta} e^{ikZ} \end{pmatrix} \equiv \begin{pmatrix} CR^{(m'-\frac{\beta}{\alpha}k)} e^{-\int_0^R A_\Theta(r')dr'} e^{im'\Theta} e^{ikZ} \\ DR^{-(m'-\frac{\beta}{\alpha}k+1)} e^{\int_0^R A_\Theta(r')dr'} e^{i(m'+1)\Theta} e^{ikZ} \end{pmatrix} \tag{4.15}$$

where $m' = m + \frac{\beta}{\alpha}k$.

The case where both C and D are nonzero cannot occur as we shall see below.

The quasi-periodicity condition (4.5) leads to the following "quantization" conditions:

$$\begin{aligned} &\text{i) When } D = 0: \qquad \alpha m' = \frac{\lambda}{2\pi} + n, \qquad n \in \mathbb{Z}, \\ &\text{ii) When } C = 0: \qquad \alpha(m'+1) = \frac{\lambda}{2\pi} + n, \qquad n \in \mathbb{Z}. \end{aligned} \tag{4.16}$$

For positive Φ , the requirement of square integrability at the origin ($r \to 0$) and at infinity ($r \to \infty$) and satisfying the boundary condition (3.7) leads to the wavefunctions

$$\Psi(R, \Theta, Z) = \begin{pmatrix} CR^m e^{-\int_0^R A_\Theta(r')dr'} e^{i(m+\frac{\beta}{\alpha}k)\Theta} e^{ikZ} \\ 0 \end{pmatrix}, \tag{4.17}$$

as well as to bounds analogous to (3.22) :

$$\begin{aligned} &\text{a) When } e^{iK} \neq 1: \qquad -\frac{1}{2} < (m' - \frac{\beta}{\alpha}k) < (\frac{\Phi}{2\pi} - 1)), \\ &\text{b) When } e^{iK} = 1: \qquad -\frac{1}{2} \leq (m' - \frac{\beta}{\alpha}k) < (\frac{\Phi}{2\pi} - 1). \end{aligned} \tag{4.18}$$

When Φ is negative, the above requirements lead to the wavefunction

$$\Psi(R, \Theta, Z) = \begin{pmatrix} 0 \\ DR^{-(m+1)} e^{\int_0^R A_\Theta(r')dr'} e^{i(m+\frac{\beta}{\alpha}k+1)\Theta} e^{ikZ} \end{pmatrix}, \tag{4.19}$$

instead, and the bounds are now the analogs of (3.25):

$$\text{c) When } e^{iK} \neq -1: \qquad -\frac{1}{2} > (m' - \frac{\beta}{\alpha}k) > \frac{\Phi}{2\pi},$$
$$\text{d) When } e^{iK} = -1: \qquad -\frac{1}{2} \geq (m' - \frac{\beta}{\alpha}k) > \frac{\Phi}{2\pi}. \tag{4.20}$$

The energy eigenvalues associated with these wavefunctions are

$$E(m,k) = \frac{k^2}{2m^*}. \tag{4.21}$$

The electronic states associated with the above wavefunctions will be loosely called zero mode electrons. The energy spectrum of these zero modes is given by

$$E = \frac{k^2}{2m^*} = \frac{\alpha^2(m'-m)^2}{2m^*\beta^2} = \frac{(\frac{\lambda}{2\pi} + n - \alpha\bar{m})^2}{2m^*\beta^2}, \tag{4.22}$$

where

$$\bar{m} = \begin{cases} m & \text{for } \Phi > 0 \ (D=0), \\ m+1 \text{ for } \Phi < 0 \ (C=0). \end{cases} \tag{4.23}$$

There are degenerate levels which can be obtained by varying the integer n or alternatively by varying m' while holding $n - \alpha m$ and hence $m' - m$ fixed.

In order to obtain the low energy effective action for the modes localized near the defect, we need to look at the behavior of the solutions near the defect. For $\Phi > \pi$ for example, the probability densities for the wave functions with $m = -\frac{1}{2}$ are peaked around the origin and for those with $m > -\frac{1}{2}$ vanish at the origin. A similar situation prevails for $\Phi < -\pi$. These peaked states are allowed only if $e^{iK} = \pm 1$. Apart from these particular states , the other states are localized at a finite distance away from the defect line. However, in a realistic situation , the defect line has a finite width and this will make some more states to be localized within the defect line, provided m is not too large and the magnetic field is large and can be treated as being uniform over the defect. This can be established from the Larmor formula,

$$r^* = \frac{m}{B} \tag{4.24}$$

where r^* is the radius of the Larmor orbit. The number of these low-energy excitations will be finite.

Though the above picture gives the single particle spectrum, one has to remember that in the many body picture for the fermions, one has to rather deal with the low energy excitations above Fermi surfaces. They can be approximated by linearizing the theory around each Fermi surface.

Now we would like to see whether these excitations are chiral as a consequence of the chirality of the screw defect. In other words, we want to know if there can be some asymmetry between excitations "above" the two Fermi surfaces given by

$$k_F = \pm\sqrt{2m^* E_F} \equiv \pm|k_F|,$$
$$E_F = \frac{k_F^2}{2m^*}. \tag{4.25}$$

The quasiparticle excitations are indeed chiral, as we can see in the following manner: We define their momenta as $\kappa \equiv k - k_F$. For excitations "above" the Fermi surfaces (which we will call particles) one has,

$$\Delta E = E - E_F \approx \frac{k_F}{m^*}\kappa > 0. \tag{4.26}$$

Thus for particle excitations at $k_F = |k_F|$, one has $\kappa > 0$ (upward or "right-movers") and for those "above" the Fermi surface at $k_F = -|k_F|$, one has $\kappa < 0$ (downward or "left movers").

However, though the quasiparticles themselves are chiral, if the situation is such that the number of upward moving and downward moving quasiparticles are equal, there will not be any net chirality. Let us investigate this point further.

For specificity, we assume that $\Phi > \pi$ *and* $\frac{\beta}{\alpha} > 0$ *in the rest of the section.* Similar considerations can be made for the remaining cases unless $\frac{\beta}{\alpha} = 0$. We will comment on the latter case later.

The relation between the linear momentum along the z-axis and the angular momentum is given by

$$m = m' - \frac{\beta}{\alpha}k \tag{4.27}$$

where m has to satisfy the bound (4.18). Also we have the fact that

$$\alpha m' = \frac{\lambda}{2\pi} + n, \qquad n \in \mathbb{Z}. \tag{4.28}$$

This shows that for a fixed value of k, the angular momenta of two neighboring states differ by

$$\Delta m' = \frac{1}{\alpha}. \tag{4.29}$$

In Figure 1 we have plotted the relation between k and m for different m's.

The lowest energy electrons occupy the levels lying *within* the region bounded by the lines $m = -\frac{1}{2}$ and $m = \frac{\Phi}{2\pi} - 1$ and $k = \pm|k_F|$, which we will call the Fermi sea hereafter.

We would like to determine the number of straight lines (which are labeled by different values of m') crossing the two Fermi surfaces. These lines correspond to the low energy excitations of the systems above the Fermi surfaces.

Note that the relation (4.27) shows that as we increase k (by applying external electric field, for instance) , m decreases for fixed m'. As we have argued earlier that m is a measure of how far away from the defect the electron is localized , this shows that the electron is drawn into the defect as k is increased. (Note that the direction of this current is dictated by the sign of $\frac{\beta}{\alpha}$ and that this transport phenomenon will not occur if $\frac{\beta}{\alpha} = 0$).

Using relations (4.27) and (4.29), one can now easily estimate the number of occupied states with a given momentum [the number of intersections of the graphs in Figure 1 with a horizontal line with a given k], provided we know the maximum and minimum value of m for the states lying within our allowed region when $k = 0$, which we denote by m_{max} and m_{min} respectively. Thus, the number of excitation branches when $k = 0$ is

$$N_0 \equiv \alpha(m_{max} - m_{min}) + 1. \tag{4.30}$$

Let us now define the following quantities

$$\begin{aligned} a &= m_{min} + \frac{1}{2}, \\ b &= m_{max} + 1 - (\frac{\Phi}{2\pi} - 1) = (m_{max} + 2 - \frac{\Phi}{2\pi}). \end{aligned} \tag{4.31}$$

The quantity a measures the horizontal distance between the line $m = -\frac{1}{2}$ and the occupied state which is just to the right of it for $k = 0$, while b measures the horizontal distance between the line $m = (\frac{\Phi}{2\pi} - 1)$ and the state which is just to the right of it for $k = 0$. (It moves into the Fermi sea when k is sufficiently increased). The value of a depends on the parameters λ and α ands hence is fixed for a given material (assuming that λ cannot be varied). On the other hand, b depends on the flux Φ and hence can be varied. Neither a nor b are functions of k_F.

Now, as we increase k from zero to a positive value, the m values for the occupied states will change and those with $m \leq -\frac{1}{2}$ will "flow" out of the spectrum. A simple counting argument shows that the number of states that will "flow" out will be given by the integer

$$N_1 = \left[\frac{k - \frac{\alpha a}{\beta}}{\frac{1}{\beta}} \right] = [\beta k - \alpha a]. \tag{4.32}$$

This equation can be obtained by noticing that the vertical spacing between two successive branches is $\Delta k = \frac{1}{\beta}$ and that the minimum value of k required to move the left-most allowed state to the left of the bound $m = -\frac{1}{2}$ is $\frac{\alpha a}{\beta}$.

At the other extreme of the allowed region, there will states moving "into" the allowed bound. The number of these incoming states can be found by arguments similar to those above. This number is given by

$$N_2 = [\beta k - \alpha b]. \tag{4.33}$$

Thus the number of branches appearing through the top Fermi surface at $k = |k_F|$ is given by

$$N_{top} = N_0 - N_1 + N_2 = \alpha(m_{max} - m_{min}) + 1 - [\beta|k_F| - \alpha a] + [\beta|k_F| - \alpha b]. \tag{4.34}$$

We can also evaluate the number of branches appearing through the bottom Fermi surface at $k = -|k_F|$, employing procedure similar to above. However, this time we have to decrease the k value from zero to a negative value $k < 0$. Decreasing the k value will make the m value for various states to increase due to the relation (4.27) since $\frac{\beta}{\alpha}$ is positive by assumption.

Consequently, states will move away from the defect and some states with $m \leq -\frac{1}{2}$ will move into the Fermi sea while some other states close to the bound $m = \frac{\Phi}{2\pi} - 1$ will " flow" out of the Fermi sea. The number of branches appearing out of the Fermi surface $k = -|k_F|$ is then given by

$$N_{bottom} = \alpha(m_{max} - m_{min}) + 1 + [\beta|k_F| + \alpha a] - [\beta|k_F| + \alpha b]. \tag{4.35}$$

Thus the difference between the number of states from the top and bottom Fermi surfaces is

$$\eta = N_{top} - N_{bottom} = [\beta|k_F| - \alpha b] + [\beta|k_F| + \alpha b] - ([\beta|k_F| - \alpha a] + [\beta|k_F| + \alpha a]). \tag{4.36}$$

This number η determines the total chirality of the excitations. Note that when $a = b$, $N_0 = N_{top} = N_{bottom}$ and $\eta = 0$. Thus, in this case the number of species remains the same irrespective of the value of $|k_F|$. However, if $a \neq b$, η can take any one of the three values , +1, 0 and -1. This is shown in Figure 2 where η is plotted as a function of $|k_F|$ for fixed values of αa and αb (which we have chosen arbitrarily). η can also change as the value of αb is changed (by varying Φ) while $|k_F|$ and αa are kept fixed. This is shown in Figure 3. So, the direction of the current due to the quasiparticles will depend on the values of $|k_F|$, αb and αa. It depends in particular on Φ.

We finally comment on the possibility $\frac{\beta}{\alpha} = 0$. Since, $|\alpha| \leq 1$, we then have $\beta = 0$ which implies the absence of the screw defect. In this case, the straight lines in Figure 1 are vertical and the net chirality η is always zero.

The zero modes dominate the contribution to the effective action for the modes localized near the defect. We will analyze the low energy effective action describing these chiral mode further in Section V.

V. TRANSPORT ALONG SOLENOIDAL DEFECTS AND ANOMALIES

We have considered a situation where there are localized states in the presence of a solenoid with flux Φ. We will now consider the response of these trapped states to a con-

stant electric field along the axis of the solenoid (that is, the defect). The low lying excitations about the Fermi surface corresponding to these states are described by massless chiral fermions localized on the defect. We proceed to discuss how their coupling to electromagnetism leads to anomalous conduction properties. To set up the relevant background for this discussion, we first recall the reasons for the $U(1)$ anomaly of chiral $(1+1)$ dimensional gauged fermionic systems.

Consider $(1+1)$ dimensional chiral , say right-handed fermions, with field, $\psi_R = \frac{1}{2}(1+\gamma_5)\psi$. The action of this fermion field coupled to a constant electric field $E(>0)$ is given by

$$S = \int dtdx\bar{\psi}_R\gamma^\mu(i\partial_\mu + A_\mu)\psi_R. \tag{5.1}$$

We choose the following γ matrix convention:

$$\gamma^t = \sigma_1; \qquad \gamma^x = -i\sigma_2, \tag{5.2}$$

so that $\gamma_5 = \gamma^t\gamma^x = \sigma_3$. The Dirac Hamiltonian for the 1+1 dimensional massless fermion is

$$\tilde{H} = \sigma_3(p - A_1) - A_0. \tag{5.3}$$

Heisenberg's equation of motion gives, for the velocity v,

$$\dot{v} = \frac{d}{dt}(p - A_1) = i[\tilde{H}, p - A_1] + \frac{\partial}{\partial\, t}(p - A_1) = -E. \tag{5.4}$$

The derivation of the chiral $U(1)$ anomaly for the action (5.1) by Nielsen and Ninomiya [14] is as follows. The density of states $\rho(v)$ for a massless $(1+1)$ dimensional particle is controlled by the following formula for its variation :

$$\delta\rho(v) = \frac{1}{2\pi}\delta v. \tag{5.5}$$

Hence the production rate of these excitations per unit length is

$$\dot{N}_R(t) = \frac{d\rho}{dt} = \frac{1}{2\pi}\dot{v} = \frac{E}{2\pi} \tag{5.6}$$

where $N_R(t)$ is the number of fermions per unit length and we have used (5.4). As these excitations carry charge, there is a non-conservation of electric charge $Q_R(t)$ carried by the right-handed fermions in the (1+1) dimensional theory, the rate of change of $Q_R(t)$ being

$$\dot{Q}_R(t) = e\dot{N}_R(t)L = -\frac{E}{2\pi}L \tag{5.7}$$

where L is the size of the sample. In this way, we obtain the $U(1)$ anomaly.

One can show in a similar way that for a left-handed chiral fermion, the rate of change of its charge $Q_L(t)$ is given by

$$\dot{Q}_L(t) = e\dot{N}_L(t)L = \frac{E}{2\pi}L \tag{5.8}$$

where $N_L(t)$ is the number density of the left-handed fermions.

Thus if there are n_1 species of right-handed fermions and n_2 species of left-handed fermions, then the rate of change of electric charge is given by

$$\frac{d}{dt}(Q_R(t) + Q_L(t)) \equiv \dot{Q}_{total} = -(n_1 - n_2)\frac{E}{2\pi}L. \tag{5.9}$$

As we are going to treat the different branches of the quasiparticle excitations as different species for the screw defect situation, one can readily see that

$$(n_1 - n_2) = \eta \tag{5.10}$$

where η is given by (4.36).

But one knows that the system as a whole has charge conservation. Therefore, when $\eta \neq 0$, it must be that charge from outside flows into or away from the defect, and there must be non-conservation of charge outside the defect too. This fact can be encoded in an anomalous Chern-Simons "effective" action, representing the electronic degrees of freedom that are not localized on the defect. The connection between the anomaly (5.7) and the Chern-Simons term is elegantly demonstrated in [9](See also [15]).

Using their results, it can be shown that the contribution appearing on the right-hand side of the equation (5.7) is cancelled by the bulk action given by

$$S_{bulk} = -\frac{\eta}{8\pi^2}\int d\phi \left[\int dt\ r dr\ dz A dA\right], \tag{5.11}$$

where η is given by the equation (4.36). The Chern-Simons three-form is being integrated here on an infinite half-plane which has the defect as the boundary, as shown in Figure 4.

The gauge variation of the Chern-Simons term produces a surface term which is exactly cancelled by the variation of the chiral anomaly on the defect [9,15], the coefficient $\frac{1}{8\pi^2}$ in (5.11) is chosen that this cancellation occurs.

The fact that the Chern-Simons coefficient is determined by the anomaly fixes of the transverse conductivity of the defect, there being an exchange of current with the bulk when an electric field is applied along the line defect. This transverse conductivity is given by $\frac{\eta}{4\pi^2} \times 2\pi = \frac{\eta}{2\pi}$, the 2π coming from the ϕ integration.[The first factor comes from varying A [15]. Recall that we have set the electric charge $e = 1$, if we had not done so, this conductivity would have been $\frac{\eta e^2}{2\pi}$]. As the value of η can change by ± 1 only, the system will behave somewhat like the integer Quantum Hall samples thought here the conductivity is bounded and the sign of the current is fixed by η .

VI. CONCLUSION

In this paper we have studied the effect of line defects on the transport properties of solids in the presence of a magnetic flux parallel to the line. This was done by describing the defects in a crystal in terms of a non-trivial metric and then studying the propagation of electrons in this background metric. We have also discussed the low energy effective action for this system. It is a $1 + 1$ dimensional chiral fermionic action localized on the defect. The coupling of this system to an external electric field parallel to the defect leads to an anomaly and induces a bulk action involving the Chern-Simons term. The resultant total action in turn leads a phenomenon similar to the transverse Hall effect with a quantized conductivity. However, the sign of the conductivity, which is proportional to η, undergoes flips as one changes the value of the magnetic flux or the Fermi momentum .

There are numerous interesting ideas suggested by the description of defects in terms of metrics and we will now discuss a few of them. It has been shown that in the background of disclination defects, electric charges experience a non-trivial force which arises due to the conical defect angle and is directed towards, or away from, the defect line. For a positive

conical angle (where a wedge has been taken out), this force turns out to be attractive (that is, towards the defect line) and leads to bound states of electrons and defects [3]. It would be interesting to see how this force is modified by the screw dislocation.

We have assumed here that the magnetic field is localized in the neighborhood of the defect. In a type-II superconductor such a scenario can actually happen. The strain energy due to the defect will force the region around the defect to be in the normal state. Then it is favorable energetically for the magnetic flux tubes to be trapped within the screw defects (if they are present in the material) [16]. This is basically due to Meissner effect. Our results, therefore, would be interesting in the study of flux-line trapping in superconductors by defects [16].

In this paper we have discussed the fact that electronic conductivity transverse to the defect is fixed in quantized units because the low energy effective theory of the electrons localized on the defects has an electromagnetic anomaly. It is known however that there is a gravitational anomaly in the same (1+1) dimensional system. It will lead to a transverse "gravitational Hall effect", and this will manifest itself in anomalous elastic and vibrational properties. Work is in progress to analyze in detail how this affects the properties of the system.

The fact that static defects can be described in terms of stationary solutions to 2+1 dimensional Einstein action for gravity with matter gives rise to the interesting possibility that the dynamics of these defects can be modeled in terms of a fully dynamical theory of gravity. It would be interesting to carry out the study of dynamics of defects in the language of quantum gravity in two and three dimensions. In particular it suggests the interesting possibility that systems with defects could provide us with analog simulations of many situations in quantum gravity that are now being studied using elaborate computer simulations.

The interplay of ideas from two widely different fields like condensed matter physics and quantum gravity can lead to lots of new results of the kind we have just discussed. It would be very interesting to use these condensed matter systems as low energy experimental probes

into what is conventionally regarded as the domain of Planck scale physics. Similar analog probes of cosmological defects have already led to rewarding results ([17])

ACKNOWLEDGMENT

We would like to thank E. Dambasuren, P. Golumbeanu, G. Jungman, S. Vaidya for furious discussions in Room 316. A.M. would also like to thank M. C. Marchetti for discussions and for pointing out reference [16]. This work was supported by the US Department of Energy under contract number DE-FG02-85ER40231.

REFERENCES

[1] F. R. N. Nabarro, *The Theory of Crystal Defects*, [Clarendon Press, Oxford (1967)].

[2] M.O. Katanaev and I.V. Volovich, Ann. Phys. **216**(1992)1 and references therein.

[3] C. Furtado and F. Moraes, Phys. Lett. **A 188** (1994) 394; C. Furtado, B. G. C. da Cunha, F. Moraes, E.R. Bezerra de Mello and V. Bezerra, Phys. Lett. **A 195** (1994) 90; F. Moraes, Mod. Phys. Lett. **A 10**(1995)2335; E. R. Bezerra de Mello , V. Bezerra, C. Furtado and F. Moraes, Phys. Rev. **D 51** (1995)7140; F. Moraes, Phys. Lett. **A 204** (1995) 399.

[4] E. Witten, Nucl. Phys. **249**(1985)1.

[5] A. Vilenkin and E. Shellard, *Cosmic Strings and Other Topological Defects*, [Cambridge University Press, Cambridge (1994).

[6] D. Boyanovsky, E. Dagotto and E. Fradkin , Nucl. Phys. **B 285**[FS19](1987)340.

[7] A.M. Kosevich, Sov. J. Low Temp. Phys. **4** (1978) 429.

[8] J. Schwinger, Phys. Rev. **128**(1962)2425. See also K. Johnson, Phys. Lett. **5** (1963) 253.

[9] C. G. Callan and J. Harvey, Nucl. Phys. **B 250**(1985)427; S. G. Naculich, Nucl. Phys. B 296(1988)837. For a concise summary, see J. Blum and J. Harvey, Nucl. Phys. **416**(1994)119.

[10] Y. Aharonov, A. Casher, Phys. Rev. **A 19** (1979) 2461. See also, R. Jackiw, Phys. Rev. **D 29**(1983)2375.

[11] M. Reed and B. Simon, *A Course in Mathematical Physics*, Vol.2, Academic Press, New York (1975).

[12] A. Moroz, Phys. Rev. **A 53** (1996) 669 and references therein.

[13] See for instance, C. Aneziris, A.P. Balachandran, M. Bordeau, S. Jo, T.R. Ramadas

and R. Sorkin, Int. J. Mod. Phys. **A 4** (1989) 5459, Sec. 2.

[14] H.B. Nielsen and M. Ninomiya, Phys. Lett. **B 130**(1983)389.

[15] A.P. Balachandran, L. Chandar and B. Sathiapalan, Nucl. Phys. **B 443**(1995)465; Int. J. Mod. Phys. **A 11** (1996) 3587.

[16] F. R. N. Nabarro and A. T. Quintanilha, in *Dislocations in Solids* vol. 5 , ed. F. Nabarro, p.193 [North Holland Publishing Comp., Amsterdam (1980)].

[17] I. Chung, R. Durrer, N.Turok and B. Yurke, Science **251** (1991)1336; M.J. Bowick, L. Chandar, E.A. Schiff and A.M. Srivastava, Science, **263**(1994)943. For a theoretical review of cosmological defect formations, see for example W. Zurek , Phys. Reports, **276** (1996) 177.

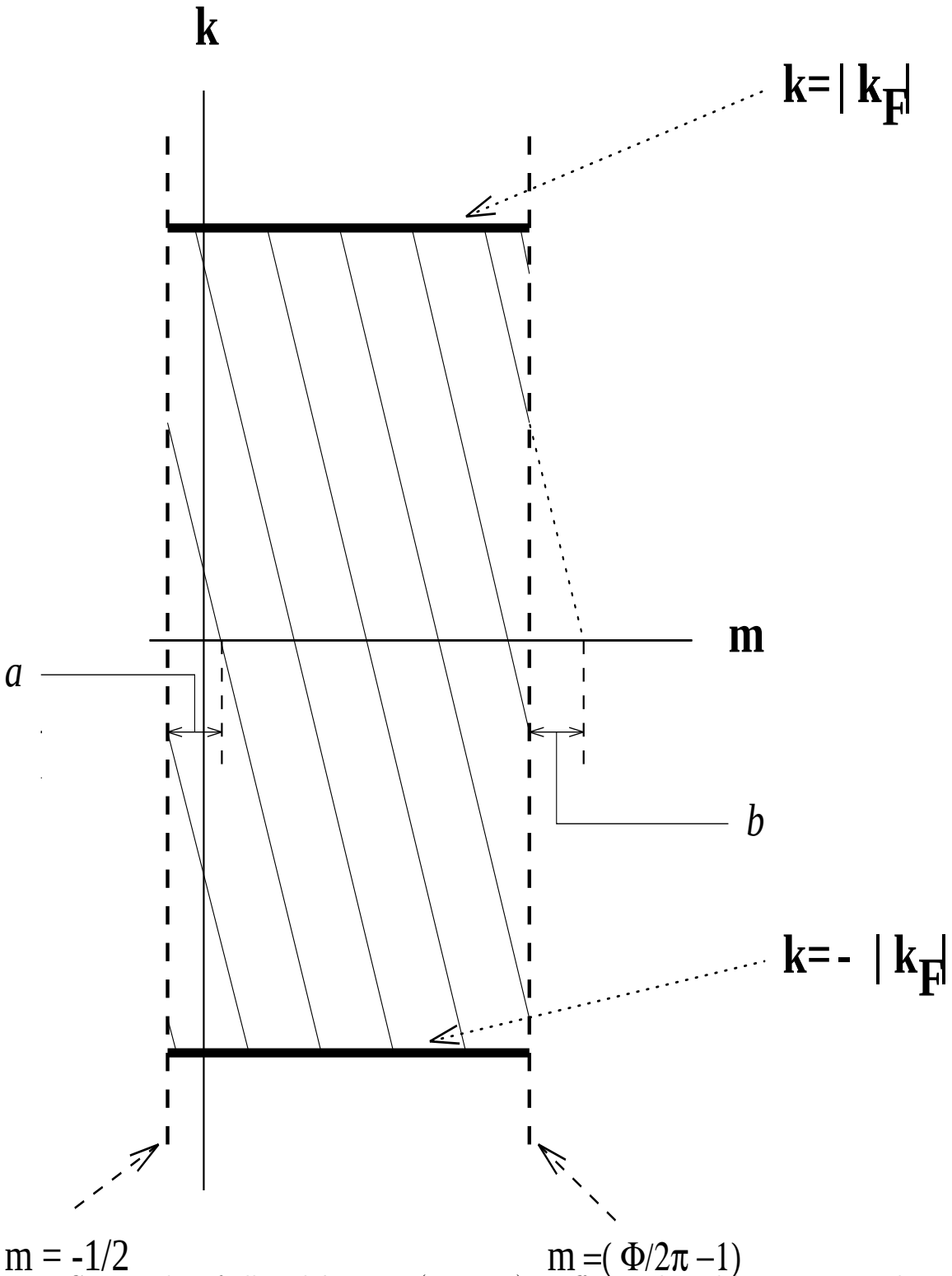

FIG. 1. Plot of allowed k vs. m ($\Phi > \pi$). Different slanted lines correspond to different values of m'.

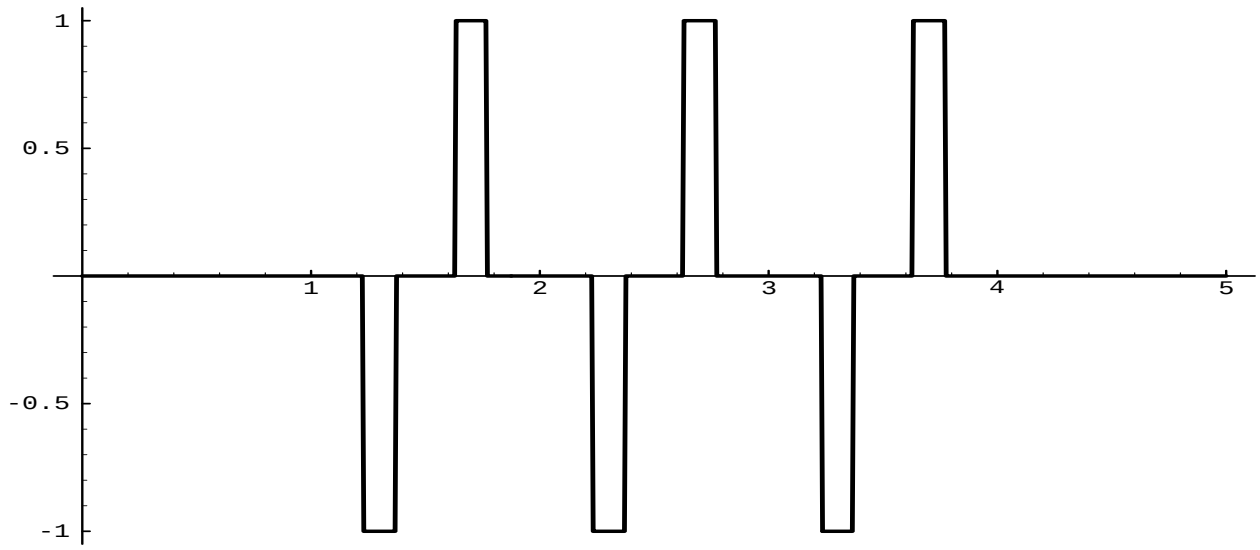

FIG. 2. Plot of η vs. $\beta|k_F|$ for $\alpha a = .23$ and $\alpha b = .37$.

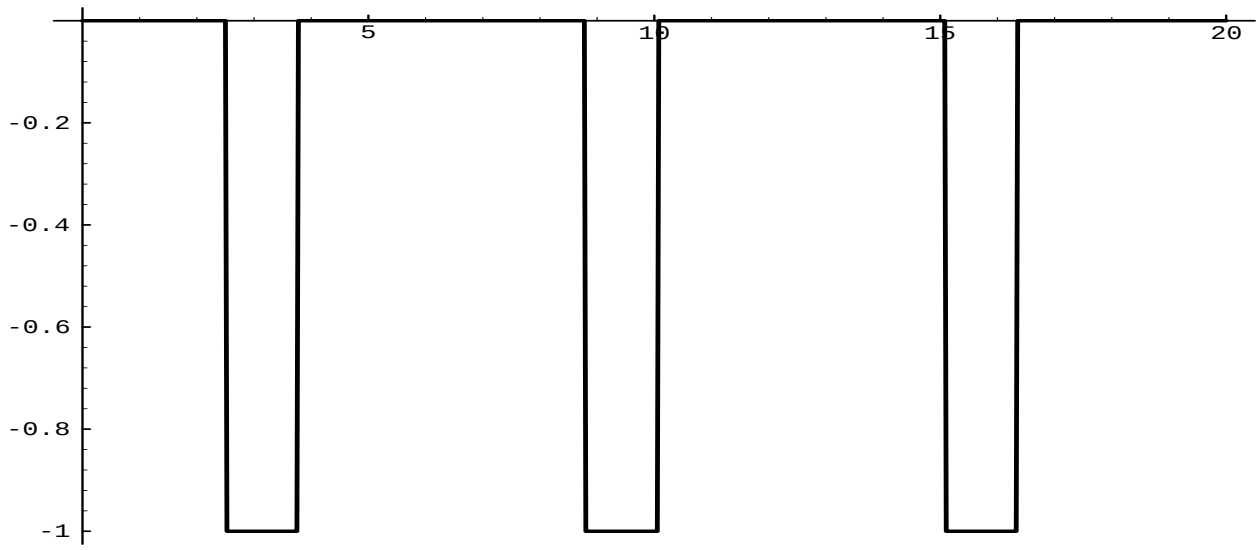

FIG. 3. Plot of η vs. Φ with $\alpha a = .37$ and $\beta|k_F| = 5.7$ and $m_{max} = 5$.

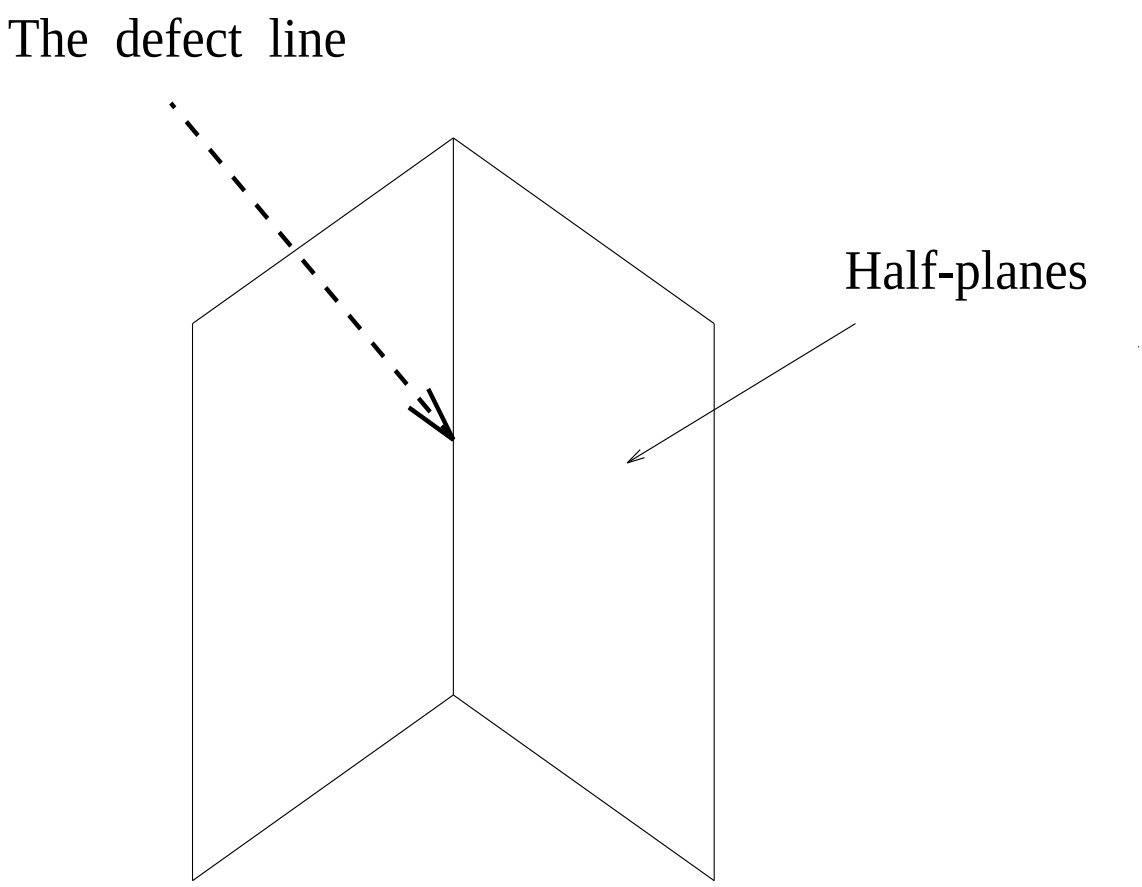

FIG. 4. Half-planes with the defect as the boundary.